


RESEARCH ARTICLE | MARCH 14 2017

# High stored energy of metallic glasses induced by high pressure

C. Wang; Z. Z. Yang; T. Ma; Y. T. Sun ; Y. Y. Yin; Y. Gong; L. Gu; P. Wen; P. W. Zhu; Y. W. Long; X. H. Yu; C. Q. Jin; W. H. Wang; H. Y. Bai

 Check for updates

*Appl. Phys. Lett.* 110, 111901 (2017)

<https://doi.org/10.1063/1.4978600>



View Online



Export Citation



## Instruments for Advanced Science

- Knowledge
- Experience
- Expertise

Click to view our product catalogue

Contact Hiden Analytical for further details:

[www.HidenAnalytical.com](http://www.HidenAnalytical.com)

[info@hiden.co.uk](mailto:info@hiden.co.uk)

Gas Analysis



- ▶ dynamic measurement of reaction gas streams
- ▶ catalysis and thermal analysis
- ▶ molecular beam studies
- ▶ dissolved species probes
- ▶ fermentation, environmental and ecological studies

Surface Science



- ▶ UHV-TPD
- ▶ SIMS
- ▶ end point detection in ion beam etch
- ▶ elemental imaging - surface mapping

Plasma Diagnostics



- ▶ plasma source characterization
- ▶ etch and deposition process reaction kinetic studies
- ▶ analysis of neutral and radical species

Vacuum Analysis



- ▶ partial pressure measurement and control of process gases
- ▶ reactive sputter process control
- ▶ vacuum diagnostics
- ▶ vacuum coating process monitoring

## High stored energy of metallic glasses induced by high pressure

C. Wang,<sup>1</sup> Z. Z. Yang,<sup>1</sup> T. Ma,<sup>1,2</sup> Y. T. Sun,<sup>1</sup> Y. Y. Yin,<sup>1</sup> Y. Gong,<sup>1</sup> L. Gu,<sup>1,3</sup> P. Wen,<sup>1</sup>  
 P. W. Zhu,<sup>2</sup> Y. W. Long,<sup>1</sup> X. H. Yu,<sup>1,a)</sup> C. Q. Jin,<sup>1</sup> W. H. Wang,<sup>1</sup> and H. Y. Bai<sup>1,a)</sup>

<sup>1</sup>Beijing National Laboratory for Condensed Matter Physics and Institute of Physics, Chinese Academy of Sciences, Beijing 100190, China

<sup>2</sup>State Key Laboratory of Superhard Materials, College of Physics, Jilin University, Changchun 130012, China

<sup>3</sup>Collaborative Innovation Center of Quantum Matter, Beijing 100190, China

(Received 18 December 2016; accepted 2 March 2017; published online 14 March 2017)

Modulating energy states of metallic glasses (MGs) is significant in understanding the nature of glasses and controlling their properties. In this study, we show that high stored energy can be achieved and preserved in bulk MGs by high pressure (HP) annealing, which is a controllable method to continuously alter the energy states of MGs. Contrary to the decrease in enthalpy by conventional annealing at ambient pressure, high stored energy can occur and be enhanced by increasing both annealing temperature and pressure. By using double aberration corrected scanning transmission electron microscopy, it is revealed that the preserved high energy, which is attributed to the coupling effect of high pressure and high temperature, originates from the microstructural change that involves “negative flow units” with a higher atomic packing density compared to that of the elastic matrix of MGs. The results demonstrate that HP-annealing is an effective way to activate MGs into higher energy states, and it may assist in understanding the microstructural origin of high energy states in MGs. *Published by AIP Publishing.* [<http://dx.doi.org/10.1063/1.4978600>]

Metallic glasses (MGs) are quenched from melts and inherit the intrinsic topological and geometrical microstructural frustrations with substantial quenched-in “defects.”<sup>1,2</sup> Confirmed by experiments and simulations,<sup>3,4</sup> MGs display microstructural heterogeneity, characterized by densely packed elastic matrix and loosely packed atomic regions in nanoscale.<sup>5</sup> The structure, size, and distribution of the denser and looser regions, which correlate with various configurations and energy states in the potential energy landscape<sup>6,7</sup> (PEL), affect the properties (e.g., strength and plasticity) of MGs.<sup>8</sup> Thus, modulating energy states through optimizing atomic configurations continues to be a challenging and current research area.

Generally, as-cast MGs naturally age or relax to lower energy states by annihilation of the free volume<sup>9</sup> or the flow unit.<sup>10</sup> Contrary to aging, MGs can also be rejuvenated to higher energy states by various mechanical<sup>11–14</sup> or thermal treatments<sup>15,16</sup> through introducing microstructural defects, which significantly modulate mechanical properties. Such high energy states of glasses can be manifested as an exothermic peak upon heating in relaxation.<sup>17</sup> Other than mechanical and thermal treatments, high pressure (HP) is also an effective and controllable way to alter microstructure, energy states, and properties of MGs. Much effort has been devoted to the pressure effect on properties of MGs, including glass transition,<sup>18</sup> crystallization,<sup>19</sup> and phase transition.<sup>20</sup> Previous study reported that structural relaxation to a lower energy state by free volume annihilation occurred during high pressure annealing (HP-annealing).<sup>18</sup> It is also reported that Ce-based MGs undergo a reversible polyamorphic phase transition under HP at room temperature (RT)<sup>21</sup> or an irreversible transition from amorphous to single crystalline states

at 25 GPa.<sup>22</sup> In this work, HP-annealing on La<sub>60</sub>Ni<sub>15</sub>Al<sub>25</sub> MG was performed. The results show that high stored energy can be achieved and preserved after unloading pressure.

Bulk La<sub>60</sub>Ni<sub>15</sub>Al<sub>25</sub> rod samples with a diameter of 3 mm were prepared by suction casting. Sample slices with 1 mm thickness were cut from the rod, and both the upper and bottom surfaces were polished to guarantee good thermal contact. These rods were cut to a length of 6 mm for the modulus and density measurements. For all samples, initialization was performed using differential scanning calorimetry (DSC) to eliminate the difference in thermal history among the as-cast samples. All the samples were heated up to 488 K into the supercooled liquid region with a heating rate of 0.33 K/s and then cooled down to RT at the same rate (see [supplementary material](#)). After initialization, the HP treatments were performed in a cubic anvil type large volume high-pressure apparatus as shown in Fig. S1, [supplementary material](#). The samples were treated under two sets of HP conditions: one is keeping the pressure (~5.5 GPa) the same while annealing at different temperatures ranging from RT to 454 K; the other is keeping the temperature (~482 K) the same while applying different pressures ranging from ambient pressure to 8.0 GPa (see details in [supplementary material](#)). The samples treated under all conditions show that crystallization did not take place during the HP treatments (see Fig. S2, [supplementary material](#)).

The structural relaxation of MGs occurred after unloading the pressure, represented by an exothermic peak below  $T_g$  in the subsequent DSC measurements. The total heat release upon heating in DSC, noted as relaxation enthalpy  $\Delta H_{rel}$ , is an indicator of the energy state of the HP-treated samples. The increase energy of MGs can be characterized by exothermal enthalpy  $\Delta H_{rel}$  in DSC measurements. Figure 1(a) shows DSC curves for samples annealed at the temperatures ranging from RT to 454 K (slightly below  $T_g$ ) under 5.5 GPa for 1 h

<sup>a)</sup> Authors to whom correspondence should be addressed. Electronic addresses: hybai@iphy.ac.cn and yuxh@iphy.ac.cn

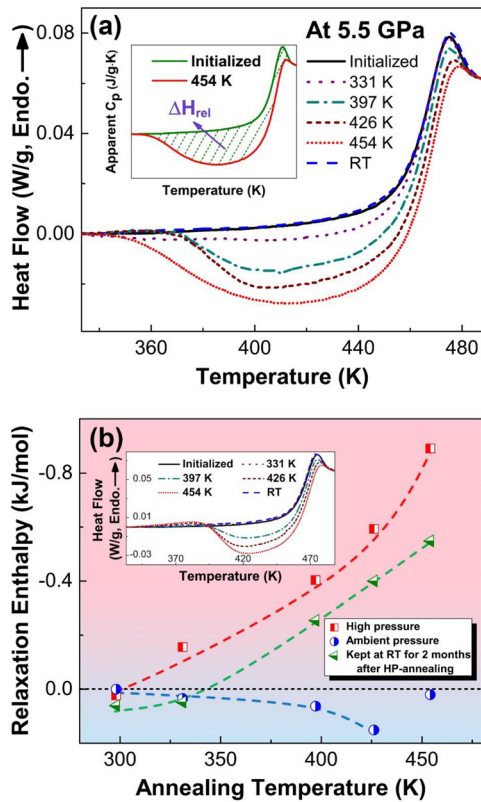


FIG. 1. High stored energy in  $\text{La}_{60}\text{Ni}_{15}\text{Al}_{25}$  bulk MG after high pressure treatments under 5.5 GPa at different temperatures. (a) DSC curves for different annealing temperatures under 5.5 GPa. Inset: The evaluation of relaxation enthalpy. (b) Relaxation enthalpy versus annealing temperature for samples tested immediately after HP-annealing and HP-annealed samples kept at RT for two months. For comparison, relaxation enthalpy of annealed samples at ambient pressure is shown. The data points are for individual samples and the changes are larger than the standard deviation of  $\pm 0.02$  kJ/mol (Error Analysis shown in the [supplementary material](#)). The dashed lines are guides to the eye. Inset: DSC curves for HP-annealed samples relaxed under ambient condition for two months.

(the curves in the whole temperature range are shown in Fig. S3, [supplementary material](#)). Glass transition temperature  $T_g$ , crystallization temperature  $T_x$ , and crystallization enthalpy are obtained to be 458 K, 523 K, and  $-5.9$  kJ/mol, respectively. The crystallization enthalpy does not change upon the experimental conditions, indicating that no crystallization occurred during HP treatments. When the samples are compressed under pressure at RT, the change of enthalpy is not observable (Fig. 1(a), blue dashed line). As the temperatures of HP-annealing increase ranging from RT to 454 K while maintaining pressure at 5.5 GPa, exothermic peaks emerge and increase with increasing temperatures of HP-annealing. The inset of Fig. 1(a) illustrates the measurements of  $\Delta H_{rel}$  after HP-annealing using the equation:  $H_{rel} = \int_{T_0}^{T_1} C_p dT$ , where  $T_0$  is a temperature ahead of exothermic relaxation peak and is set as 333.15 K and  $T_1$  is a temperature in the supercooled liquid region and is set as 488.15 K.  $\Delta C_p$  is the difference between the specific heats of the initialized and HP-annealed samples. The exothermic enthalpy versus annealing temperature prior to measuring the stored enthalpy is presented in Fig. 1(b). A relaxation enthalpy of 0.9 kJ/mol is obtained for the sample treated at 454 K under 5.5 GPa, which is three times larger than that of the rejuvenated samples treated by thermal cycling,<sup>15</sup> and similar to those treated by

plastic deformation.<sup>12,13</sup> The HP-annealed samples were kept at RT for two months, and the high stored energy has been partially released, yet major part of it remained (inset of Fig. 1(b)). On the contrary, for the MGs annealed at the same temperature under ambient pressure, the thermal process in DSC is slightly endothermic (Fig. 1(b) and Inset (a) of Fig. 2(b)), which is consistent with previous studies.<sup>23</sup> The aging effect at the same temperature under ambient pressure suggests that HP plays a crucial role in the achievement of high stored energy in MGs.

To study the pressure effect, the MGs were annealed at the same temperature of 426 K for 1 h under different pressures: ambient pressure, 1.0, 2.2, 4.0, 5.5, and 8.0 GPa, respectively. The DSC measurements after HP-annealing are presented in Fig. 2(a). When pressure was relatively lower (ambient pressure and 1.0 GPa), the MG samples aged to a lower energy state. As the pressure increased to 2.2 GPa, an exothermic peak appeared, the intensity of which increased with increasing pressure and finally reached a maximum at 8.0 GPa. Correspondingly, the exothermal enthalpy (Fig. 2(b)) increases with increasing pressure and reaches 0.9 kJ/mol at 8.0 GPa. For the samples treated under different pressures at RT, no obvious change happened in DSC measurements (Inset (b) of Fig. 2(b)), suggesting that high temperature is also a necessary condition for achieving high stored energy of MGs. Therefore, the high stored energy of MGs is attributed to the coupling effect of high pressure and high temperature.

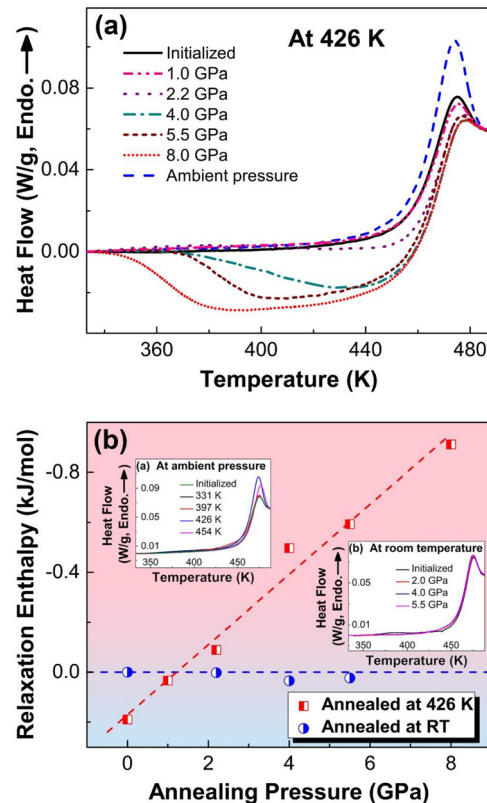


FIG. 2. High stored energy in  $\text{La}_{60}\text{Ni}_{15}\text{Al}_{25}$  bulk MG after treatments at 426 K under different pressures. (a) DSC curves for different pressures at 426 K. (b) Relaxation enthalpy versus annealing pressure for samples treated at high temperature (426 K) and RT (298 K) under different pressures. The dashed lines are guides to the eye. Inset (a), (b), DSC curves for samples annealed at different temperatures under ambient pressure and under different pressures at RT, respectively.

Figure 3 shows schematic HP-annealing temperature dependent enthalpy of glasses and supercooled liquids under different pressures. During sub- $T_g$  annealing, the enthalpy of MGs moves towards the equilibrium state, which is the extrapolated line of the supercooled liquidus. When the pressure increases to a certain extent, the enthalpy of supercooled liquid will increase<sup>24</sup> (upper black dashed line in Fig. 3), which is confirmed by Molecule Dynamics simulations (see Fig. S5, [supplementary material](#)). As a result, there is an intersection temperature,  $T_{in}$ , between the line of enthalpy for glass under ambient pressure (black solid line) and the line extrapolated from the supercooled liquid under HP (black dashed line). When annealing temperature is higher than  $T_{in}$ , the enthalpy will increase towards (red arrow line) the HP equilibrium state upon HP-annealing. However, aging still dominates the process under ambient pressure and the enthalpy decreases (blue arrow line). If HP-annealing temperature is below  $T_{in}$ , the enthalpy will decrease towards the extrapolated liquidus for HP (light blue dashed arrow line), suggesting that both high temperature and HP are necessary conditions for the achievement of high energy states.

The high stored energy induced by HP-annealing can also be interpreted by the PEL theory.<sup>6,7</sup> During sub- $T_g$  annealing, the MG has potential to jump across the energy barrier, fall into a local minimum with lower energy, and finally relax to an ideal glass after being annealed for sufficient time due to ergodicity.<sup>25</sup> Confirmed by previous studies, strain can induce disappearances of energy minima<sup>26,27</sup> and the energy of the system increased to a higher level after a large strain cycle.<sup>28</sup> In this case, the shape of the PEL has been vastly changed, and the system relaxes into a local minimum far from the initial state, which signifies that the final configuration has changed greatly. After strain recovering, the preserved configuration may locate in the minimum with higher energy than that of initial configuration.<sup>28</sup> In the case

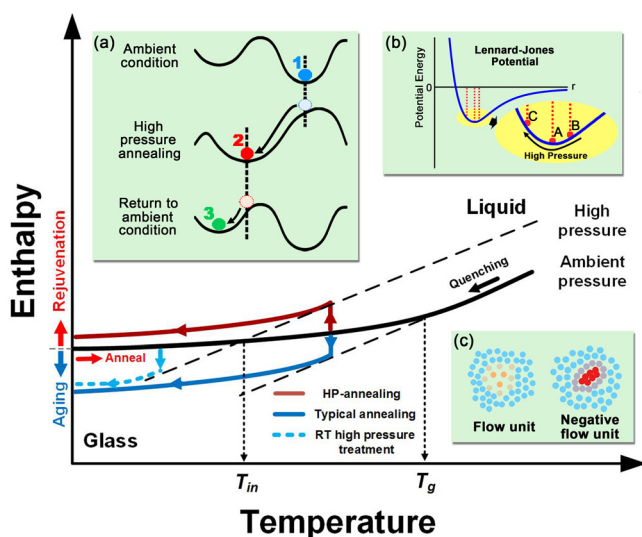


FIG. 3. Schematic of temperature dependent enthalpy change of the MGs and supercooled liquids under different HP-annealing conditions. The energy state of MGs could be altered upon HP-annealing below glass transition temperature. Inset: (a) PEL changes for MGs under different pressures upon HP-annealing. (b) Sketch of the Lennard-Jones-like potential. A, B and C schematically denote the average interatomic distances upon different pressures. (c) The difference between “flow units” and “negative flow units.”

of HP-annealing, HP alters the PEL dramatically. As displayed in Inset (a) of Fig. 3, a configuration in PEL varies vastly under HP. Accordingly, the energy of MG annealed under HP could be kept in a local minimum in the HP-PEL with a configuration quite different from the initial one (from state 1 to 2). After unloading the pressure, the configuration favored under HP is no longer preferred, but at ambient condition, the temperature is too low to provide energy to overcome the energy barrier, and no notable atomic rearrangement can take place after unloading at RT. Consequently, the MG can only reside into a local minimum with a similar configuration to that of HP (from energy state 2 to 3). Therefore, the higher energy state can be preserved after HP-annealing in the PEL theory.

Generally, high pressure promotes atomic rearrangement in short range. When pressure is low, free volume annihilation dominates the process and results in aging.<sup>18,29</sup> However, when the pressure is high, the MGs are compressed greatly, the atoms will rearrange into configurations with higher atomic packing density. As shown in Fig. 2(b), the energy of MGs decreases under lower pressure (ambient pressure and 1 GPa) but increases with increasing pressure. It can also be interpreted by the Lennard-Jones-like potential (Fig. 3 inset (b)) that when the interatomic distance is larger or smaller than the critical distance (A) of the bottom of the potential well, the potential energy will increase. During HP-annealing, the interatomic distance will first decrease towards the critical distance (from B to A), leading to free volume annihilation that corresponds to aging. When the pressure further increases, the interatomic distance will decrease to the left (from A to C), leading to a higher potential energy and a further densification of MGs.

To verify the above assumption, we measured the density and elastic modulus of the HP-annealed MGs. Unlike previous results, where rejuvenation in energy states usually causes a decrease in density and elastic modulus,<sup>12,15</sup> in the present study a reverse trend is observed. After annealing at 454 K under 5.5 GPa for 1 h, the density increases by 1.09% (from 5.82 g/cm<sup>3</sup> to 5.88 g/cm<sup>3</sup>). The elastic and shear moduli increase by 2.65% (from 38.4 GPa to 39.4 GPa) and 3.15% (from 14.3 GPa to 14.8 GPa), respectively. From previous reports, the high energy stored in MGs originates from microstructural defects of flow units,<sup>10</sup> which usually act like “soft spots” with a lower atomic packing density and a lower coordination.<sup>30,31</sup> However, in HP-annealing, the high stored energy is accompanied by densification, implying that a different microstructural origin exists.

To investigate structural origin of the high stored energy by HP-annealing, double aberration corrected scanning transmission electron microscopy (Cs-STEM) experiments were performed. Samples were polished with a Twin-jet Electropolishing device cooled by liquid nitrogen below  $-40^{\circ}\text{C}$ . All the scanning parameters were kept constant (see [supplementary material](#)). Figures 4(a) and 4(b) show the Cs-STEM dark-field images of the distribution of metallic atoms in the initialized and HP-annealed samples, respectively. The yellow spots represent relatively denser packed regions and blue regions denote looser packed regions. Figures 4(c) and 4(d) show the atomic resolution Cs-STEM images of the same area of Figs. 4(a) and 4(b), in which

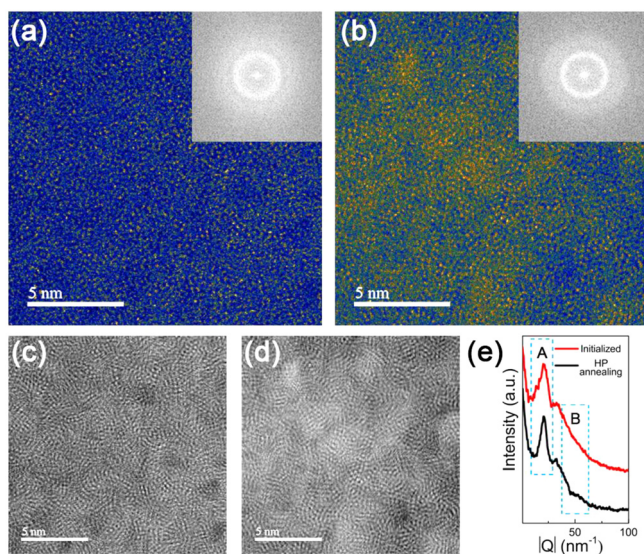


FIG. 4. Cs-STEM images of  $\text{La}_{60}\text{Ni}_{15}\text{Al}_{25}$  samples. (a) and (b), Colored Cs-high-angle annular dark-field (HAADF) STEM images of the projective distribution of metallic atoms in both initialized and HP-annealed samples with  $16.384 \times 16.384 \text{ nm}^2$  scan range, respectively. Insets show the corresponding diffraction patterns of (a) and (b) obtained by FFT. (c) and (d) Filtered atomic resolution Cs-STEM images of the same area of (a) and (b). (e) Integrated intensity profile of FFT images in (a) and (b). A and B denotes the differences between samples.

random distribution of atoms is clearly visible. All images show amorphous structures, which are consistent with XRD results. However, compared with the initialized sample, the HP-annealed sample shows much larger regions with higher atomic packing density (yellow spots in Fig. 4(b)). In addition, in the Fast Fourier Transformation (FFT) images (inset of Figs. 4(a) and 4(b)), the HP-annealed sample displays a slightly sharper ring than that of the initialized sample, implying an ascending trend of local structural ordering. This is also consistent with the secondary ring outside the halo ring where there is a sudden leap in intensity in the FFT image of HP-annealed sample. The intensity of the FFT images is integrated<sup>32</sup> (Fig. 4(e)), and it has two distinct features, marked as A and B. For the HP-annealed sample, the A peak is narrower, indicating a trend to a higher short range ordering. The position of B locates at high Q value, which corresponds to a short interatomic distance. There is a hump around B, indicating that more atoms possess shorter interatomic distance in the HP-annealed sample than that in the initialized sample. These atoms contribute to higher atomic packing density, which is the structural origin of high stored energy by HP-annealing.

The high stored energy in MGs is usually accompanied by an increase in flow units with lower atomic packing densities containing free volumes. However, the high stored energy induced by HP-annealing originates from clusters with higher atomic packing density. They are termed as negative flow units, which possess higher density and higher energy. Opposite to normal flow units, negative flow units contain anti-free volumes that have been confirmed by high-energy X-ray diffraction<sup>33,34</sup> and experimentally observed in colloidal system.<sup>35</sup> During HP-annealing, pressure first leads to free volume annihilation, resulting in structural relaxation to lower energy states and increase in

density, as happened in aging. When the pressure increases to a certain value, the negative flow units are produced accompanied by a further increase in density, which has also been confirmed by recent simulation work from Miyazaki *et al.*, in which systematic studies on thermal rejuvenation and compressive effect under hydrostatic pressure have been reported.<sup>36</sup> According to the experimental observations, the flow units change from positive to zero, and finally to a negative value, simultaneously the density and modulus increase continuously.

In summary, the MGs can be activated to high energy states by HP-annealing below  $T_g$  due to the coupling effects of pressure and temperature. The high stored energy is accompanied by an increase in density and modulus due to the formation of the negative flow units, which have a higher atomic packing density. The difference between PELs under HP and ambient pressure results in such change. This study enriches the traditional theories of flow units with a lower atomic packing density and shows experimentally the existence of negative flow units by HP treatments. Compared to conventional rejuvenation, the HP-induced high stored energy demonstrates the unique features: higher density, modulus and higher energy with negative flow units.

See [supplementary material](#) for experimental details, error analysis method and data for: XRD structure and Molecule Dynamics results of potential energy under different pressures.

The discussions with Y. Z. Li, T. P. Ge, T. F. Pei and R. J. Xue, and experimental assistance by L. Han are appreciated. The work was supported by NSF of China (Nos. 51271197, 51271195, 51522212 and 51421002), MOST 973 Program (Nos. 2015CB856800, 2012CB932704 and 2014CB921002) and the Strategic Priority Research Program of Chinese Academy of Sciences (Grant No. XDB07030200).

<sup>1</sup>D. Turnbull and M. H. Cohen, *J. Chem. Phys.* **34**, 120 (1961).

<sup>2</sup>M. W. Chen, *Annu. Rev. Mater. Res.* **38**, 445 (2008).

<sup>3</sup>Y. H. Liu, D. Wang, K. Nakajima, W. Zhang, A. Hirata, T. Nishi, A. Inoue, and M. W. Chen, *Phys. Rev. Lett.* **106**, 125504 (2011).

<sup>4</sup>A. Widmer-Cooper, H. Perry, P. Harrowell, and D. R. Reichman, *Nat. Phys.* **4**, 711 (2008).

<sup>5</sup>T. Egami, K. Maeda, and V. Vitek, *Philos. Mag. A* **41**, 883 (1980).

<sup>6</sup>F. H. Stillinger, *Science* **267**, 1935 (1995).

<sup>7</sup>P. G. Debenedetti and F. H. Stillinger, *Nature* **410**, 259 (2001).

<sup>8</sup>W. H. Wang, *Prog. Mater. Sci.* **57**, 487 (2012).

<sup>9</sup>F. Spaepen, *Acta Metall.* **25**, 407 (1977).

<sup>10</sup>Z. Lu, W. Jiao, W. H. Wang, and H. Y. Bai, *Phys. Rev. Lett.* **113**, 045501 (2014).

<sup>11</sup>H. B. Ke, P. Wen, H. L. Peng, W. H. Wang, and A. L. Greer, *Scr. Mater.* **64**, 966 (2011).

<sup>12</sup>F. Meng, K. Tsuchiya, I. Seiichiro, and Y. Yokoyama, *Appl. Phys. Lett.* **101**, 121914 (2012).

<sup>13</sup>M. Stolpe, J. J. Kruzic, and R. Busch, *Acta Mater.* **64**, 231 (2014).

<sup>14</sup>A. Concustell, F. O. Mear, S. Surinach, M. D. Baro, and A. L. Greer, *Philos. Mag. Lett.* **89**, 831 (2009).

<sup>15</sup>S. V. Ketov, Y. H. Sun, S. Nachum, Z. Lu, A. Chicchi, A. R. Beraldin, H. Y. Bai, W. H. Wang, D. V. Louzguine-Luzgin, M. A. Carpenter, and A. L. Greer, *Nature* **524**, 200 (2015).

<sup>16</sup>M. Wakeda, J. Saida, J. Li, and S. Ogata, *Sci. Rep.* **5**, 10545 (2015).

<sup>17</sup>Y. H. Sun, A. Concustell, and A. L. Greer, *Nat. Rev. Mater.* **1**, 16039 (2016).

<sup>18</sup>H. J. Jin, X. J. Gu, P. Wen, L. B. Wang, and K. Lu, *Acta Mater.* **51**, 6219 (2003).

<sup>19</sup>F. Ye and K. Lu, *Acta Mater.* **47**, 2449 (1999).

- <sup>20</sup>Y. Fang and J. Jiang, *J. Non-Cryst. Solids* **358**, 3212 (2012).
- <sup>21</sup>H. W. Sheng, H. Z. Liu, Y. Q. Cheng, J. Wen, P. L. Lee, W. K. Luo, S. D. Shastri, and E. Ma, *Nat. Mater.* **6**, 192 (2007).
- <sup>22</sup>Q. Zeng, H. Sheng, Y. Ding, L. Wang, W. Yang, J.-Z. Jiang, W. L. Mao, and H.-K. Mao, *Science* **332**, 1404 (2011).
- <sup>23</sup>Z. G. Zhu, P. Wen, D. P. Wang, R. J. Xue, D. Q. Zhao, and W. H. Wang, *J. Appl. Phys.* **114**, 083512 (2013).
- <sup>24</sup>R. S. Jones and N. W. Ashcroft, *J. Chem. Phys.* **80**, 3328 (1984).
- <sup>25</sup>H. B. Yu, Y. Luo, and K. Samwer, *Adv. Mater.* **25**, 5904 (2013).
- <sup>26</sup>D. L. Malandro and D. J. Lacks, *Phys. Rev. Lett.* **81**, 5576 (1998).
- <sup>27</sup>D. J. Lacks, *Phys. Rev. Lett.* **87**, 225502 (2001).
- <sup>28</sup>D. J. Lacks and M. J. Osborne, *Phys. Rev. Lett.* **93**, 255501 (2004).
- <sup>29</sup>A. Vandenbeukel and J. Sietsma, *Acta Metall. Mater.* **38**, 383 (1990).
- <sup>30</sup>Y. Q. Cheng and E. Ma, *Prog. Mater. Sci.* **56**, 379 (2011).
- <sup>31</sup>W. Dmowski, T. Iwashita, C. P. Chuang, J. Almer, and T. Egami, *Phys. Rev. Lett.* **105**, 205502 (2010).
- <sup>32</sup>J. L. Labar, *Ultramicroscopy* **103**, 237 (2005).
- <sup>33</sup>T. Egami, *Prog. Mater. Sci.* **56**, 637 (2011).
- <sup>34</sup>W. Dmowski, Y. Yokoyama, A. Chuang, Y. Ren, M. Umemoto, K. Tsuchiya, A. Inoue, and T. Egami, *Acta Mater.* **58**, 429 (2010).
- <sup>35</sup>X. N. Yang, R. Liu, M. C. Yang, W. H. Wang, and K. Chen, *Phys. Rev. Lett.* **116**, 238003 (2016).
- <sup>36</sup>N. Miyazaki, M. Wakeda, Y. J. Wang, and S. Ogata, *NPJ Comput. Mater.* **2**, 16013 (2016).